Weighted reconstruction methodology for optoacoustic tomographic imaging of heterogeneous acoustic samples

X Luís Deán-Ben, Vasilis Ntziachristos and Daniel Razansky *

Institute for Biological and Medical Imaging, Technical University of Munich and Helmholtz Center Munich, Ingolstädter Landstraße 1, 85764 Neuherberg, Germany.

ABSTRACT

Some biological samples contain strongly mismatched tissues such as bones or lungs that generally produce acoustic reflections and scattering, leading to consequent image distortion if the reconstruction is performed by assuming an acoustically homogeneous medium. A weighted optoacoustic reconstruction procedure based on statistical principles is presented herein to tomographically image tissues with strong acoustic mismatch. The procedure is based on weighting the contribution of the collected optoacoustic signals to the reconstruction with the probability that they are not affected by reflections or scattering. Since such probability depends on the available information about the distribution of optical absorbers, an iterative procedure in which the reconstructted images are used to recalculate the weighting values is presented in this work. The benefit of the reconstruction procedure described herein is showcased by reconstructing a phantom containing a straw filled with air, which mimicks air-gaps in actual biological samples.

Keywords: Optoacoustic tomography, photoacoustic tomography, ultrasonic scattering, ultrasonic reflections, acoustic heterogeneities

1. INTRODUCTION

Optical imaging is acknowledged as a very versatile tool in biological studies involving small animals and selected clinical applications.[1,2] The main reason for this is the high and specific contrast given by the interaction of optical photons with intrinsic or extrinsically administered molecules, making optical imaging techniques very suitable for molecular imaging applications due to the large range of optical probes available.

Macroscopic optical imaging (penetration depths in the order of several millimeters to centimeters in biological tissues) is however hampered by the strong scattering of photons as they propagate in tissues, which significantly reduces the achievable resolution. The limited resolution achievable with optical methods in whole-body small animal imaging has shifted the attention of the diffuse optical community to optoacoustic techniques, which preserve the advantages derived from optical excitation of molecules but render higher ultrasonic resolution.[3,4]

The high optoacoustic resolution at depths beyond the diffusive limit of light stems from the low scattering of sound, as compared to photons, within biological tissues. In this way, acoustic distortion is not considered in most reconstruction algorithms assuming an ideal acoustic medium with uniform density and speed of sound.[5–8] However, some biological samples contain strongly mismatched tissues such as bones, lungs or other air cavities that generally produce acoustic reflections or scattering, with a consequent image distortion and artefacts if the reconstruction is done with standard optoacoustic reconstruction algorithms.[9] The propagation of acoustic waves is also affected by small variations in the speed of sound present in soft tissues (typically below 10% with respect to the speed of sound in water) as well as by acoustic attenuation, which plays a role when imaging at high ultrasonic frequencies.[10–13]

We have recently developed a weighted reconstruction procedure based on statistical principles that allows minimizing the artefacts associated to acoustic propagation distortion phenomena.[9] In this way, by weighting the contribution of different signals with the probability that they are not affected by distortion one can achieve a better quality in the reconstructed images. In a first order approximation, late optoacoustic responses are being weighted less than signals arriving earlier. Moreover, the statistical procedure establishes the basis to

*E-mail: dr@tum.de

determine which part of the signals must be weighted if more structural information regarding the distribution of optical absorbers and acoustic scatterers or reflectors is available.[14,15] The methodology is applicable to different reconstruction algorithms such as back-projection or model-based inversion schemes. Herein, model-based inversion is iteratively weighted by considering the reconstructed optical absorption in each iteration. The distribution of acoustic scatterers can also be considered to further improve the quality of the images.

In this work, we showcase the performance of the iterative reconstruction procedure by imaging a tissue-mimicking agar phantom containing a straw filled with air, which mimicks air-gaps in actual biological samples. The benefits of using structural information on the statistically-based weighting procedure are then showcased.

2. THEORY

2.1 Probability of signal distortion due to acoustic reflections or scattering

Optoacoustic reconstruction algorithms are generally derived by considering an acoustic medium with constant density and speed of sound, in a way that the acoustic waves generated at a certain point $\boldsymbol{r}'$ propagate without distortion until the measuring position $\boldsymbol{r}$ with a time-of-flight $t = |\boldsymbol{r} - \boldsymbol{r}'|/c$. However, when acoustic reflections or scattering take place within the sample, the ultrasonic waves are in general delayed, so that they interfere at the measuring point with other waves generated at farther locations. Thereby, not all of the signals recorded at the different positions are equally adequate for reconstructing the optical absorption at $\boldsymbol{r}'$. Depending on the available information regarding the distribution of optical absorbers and acoustic scatterers on the imaging sample, we can establish which part of the signals are more likely to be distorted by reflected or scattered ultrasonic waves.

We define the probability $P_r^i(t_j)$ that a reflected or scattered wave with unit amplitude (in arbitrary units) is detected by the i-th transducer at time t_j. $P_{r,dist}^i(t_j)$ is defined as the probability that the wave, measured with the i-th transducer at instant t_j, is distorted by a reflected or scattered wave, which in practice is the case when the scattered or reflected wave is above the noise level. We consider that $P_{r,dist}^i(t_j)$ is proportional to $P_r^i(t_j)$. Then, according to Bayes' theorem, $P_{r,dist}^i(t_j)$ can be expressed as[9]

$$P_{r,dist}^i(t_j) = k_1 \int_{\mathrm{A}} P_{r,dist}^i(t_j|\boldsymbol{r}') f_E(\boldsymbol{r}') d\boldsymbol{r}', \tag{1}$$

where $P_{r,dist}^i(t_j|\boldsymbol{r}')$ is the conditional probability that the signal measured with the i-th transducer is distorted at t_j given that all the energy absorbed by the sample is entirely absorbed at $\boldsymbol{r}'$. A is an area covering the imaging sample where optical absorption takes place. $f_E(\boldsymbol{r}')$ is the probability density function corresponding to the location at which a differential of energy is absorbed. If the optical absorption $H(\boldsymbol{r}')$ is known, $f_E(\boldsymbol{r}')$ is proportional to $H(\boldsymbol{r}')$, so that Eq. 1 can be expressed as

$$P_{r,dist}^i(t_j) = k_2 \int_{\mathrm{A}} P_{r,dist}^i(t_j|\boldsymbol{r}') H(\boldsymbol{r}') d\boldsymbol{r}', \tag{2}$$

Furthermore, if and area B containing all the acoustic scatterers or reflectors is known $P_{r,dist}^i(t_j)$ can more accurately be determined. Thus, if it is assumed that only one scattering or reflection event takes place, Eq. 2 can be expressed as

$$P_{r,dist}^i(t_j) = k_3 \int_{\mathrm{A}} \left[\int_{\mathrm{B}} H(\boldsymbol{r}') \delta\left(t_{\mathrm{r}}^i(\boldsymbol{r}', \boldsymbol{r}'') - t_j\right) d\boldsymbol{r}'' \right] d\boldsymbol{r}', \tag{3}$$

In order to estimate the shape of $P_{r,dist}^i(t_j)$ the Monte Carlo method is used, so that n pairs of points $(\boldsymbol{r}', \boldsymbol{r}'')$ in A and B are randomly generated and the corresponding values of $t_{\mathrm{r}}^i(\boldsymbol{r}', \boldsymbol{r}'')$ are calculated. If the value of n is large enough, the histogram of $t_{\mathrm{r}}^i(\boldsymbol{r}', \boldsymbol{r}'')$ faithfully represents the shape of $P_{r,dist}^i(t_j)$.

2.2 Weighted model-based reconstruction

The model-based reconstruction procedure employed herein is based on a discretization of the analytical solution for optoacoustic sources confined in the imaging plane, which is applicable when cylindrically-focused transducers are used to collect the optoacoustic signals.[16] In this way, the optoacoustic pressure at a point $\boldsymbol{r}_i$ and at an instant t_j can be expressed as a linear combination of the absorption $H(\boldsymbol{r}'_k)$ at the grid of points representing the reconstruction region of interest (ROI), i.e.,

$$p(\boldsymbol{r}_i, t_j) = \sum_{k=1}^{N} a_k^{ij} H(\boldsymbol{r}'_k). \tag{4}$$

If the pressure for P positions of the transducer and for I instants is considered, a system of linear equations can be formulated, which is expressed in a matrix form as

$$\mathbf{p} = \mathbf{A}_{\mathrm{M}}\mathbf{H}. \tag{5}$$

Eq. 5 corresponds to the forward model, in which the theoretical pressure for a set of detector positions and instants $\mathbf{p}$ is calculated as a function of the absorbed energy in the pixel positions $\mathbf{H}$, being $\mathbf{A}_{\mathrm{M}}$ the model-matrix.

The optoacoustic reconstruction is performed by minimizing the mean square difference between the theoretical pressure $\mathbf{p}$ and the measured pressure $\mathbf{p}_{\mathrm{m}}$, i.e.,

$$\mathbf{H}_{\mathrm{sol}} = \underset{\mathbf{H}}{\operatorname{argmin}} \left\| \mathbf{p}_{\mathrm{m}} - \mathbf{A}_{\mathrm{M}}\mathbf{H} \right\|^2. \tag{6}$$

In order to minimize distortion due to acoustic scattering or reflections, the reconstruction procedure is weighted with the probability $P_d^i(t_j) = 1 - P_{r,dist}^i(t_j)$ that the detected signal corresponds to direct wave propagation between the excitation and detection points. In this way, a diagonal matrix $\mathbf{W}$ with elements $P_d^i(t_j)$ is used to weight the linear system of equations, which is modified as

$$\mathbf{W}\mathbf{p} = \mathbf{W}\mathbf{A}_{\mathrm{M}}\mathbf{H}, \tag{7}$$

so that the reconstruction is then made by solving a mean square difference minimization problem equivalent to Eq. 6, given by

$$\mathbf{H}_{\mathrm{sol}} = \underset{\mathbf{H}}{\operatorname{argmin}} \left\| \mathbf{W}\mathbf{p}_{\mathrm{m}} - \mathbf{W}\mathbf{A}_{\mathrm{M}}\mathbf{H} \right\|^2. \tag{8}$$

The solution of Eq. 8 is calculated by means of the LSQR algorithm, in which the sparsity of the model matrix is exploited to make a fast reconstruction.

As the calculation of $\mathbf{W}$ depends on the optical absorption distribution (Eq. 3), we suggest herein an iterative procedure in which the solution $\mathbf{H}_{\mathrm{sol}}$ for each iteration is used as the optical absortion to estimate $\mathbf{W}$ in the next iteration.

3. MATERIALS AND METHODS

A tissue-mimicking agar phantom (1.3% agar powder by weight) was used in the experiments. Black India ink and Intralipid were added to the agar solution in order to simulate the background tissue optical absorption and scattering. Specifically, 0.002% by volume of ink and 1.2% by volume of Intralipid were added, corresponding, respectively, to an optical absorption coefficient of $\mu_a = 0.2\ \mathrm{cm}^{-1}$ and a reduced scattering coefficient of $\mu'_s = 10\ \mathrm{cm}^{-1}$. An insertion with higher optical absorption ($\mu_a \approx 2\ \mathrm{cm}^{-1}$) was included in a region close to the surface of the phantom. Furthermore, a hollow cylindrical cavity (a straw filled with air) was positioned close to the absorber, so that the artefacts associated to ultrasonic reflections appear in a region close to the centre of the image.

The experimental system used to image the phantoms is described in Ref. 17. Basically, the output laser beam was shaped to attain ring-type uniform illumination on the surface of the phantoms. The laser source is an optical parametric oscillator (OPO) laser with 10 Hz pulse repetition and a tunable optical wavelength that was set to 750 nm in the experiments. An array of 256 cylindrically-focused ultrasonic transducers with a central frequency of 5 MHz and a focal length of approximately 40 mm was employed to collect the optoacoustic signals, which were averaged 20 times and a band-pass filtered with cut-off frequencies 0.1 and 7 MHz.

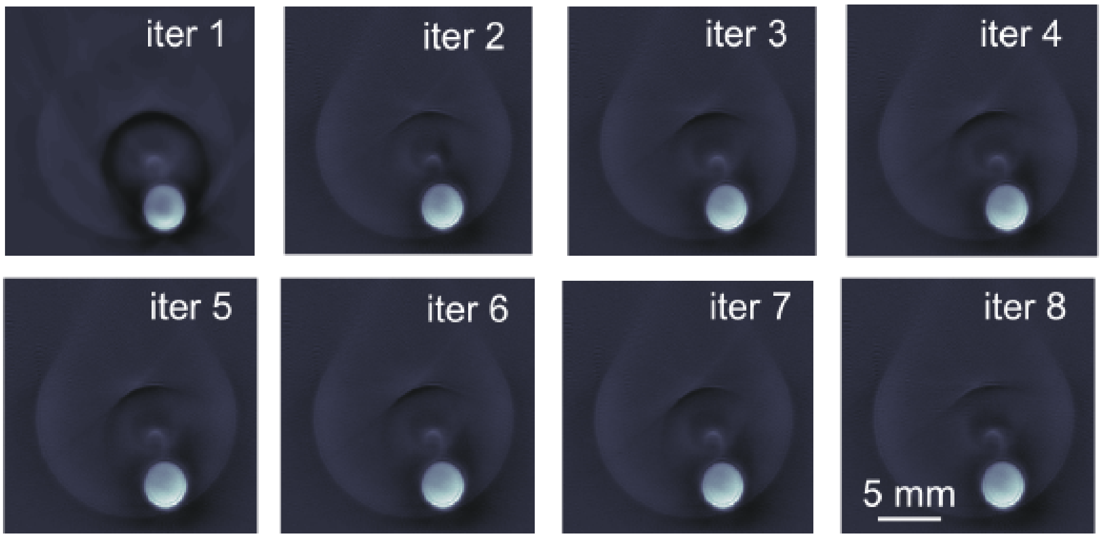

Figure 1. Eight first iterations of the weighted reconstruction procedure when no information about the imaging sample is *a priori* available.

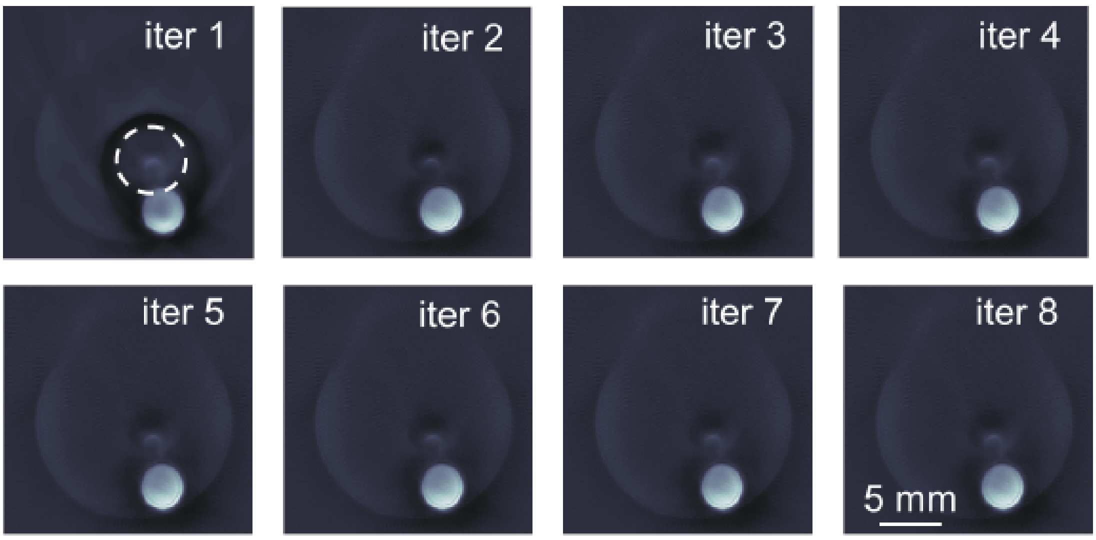

Figure 2. Eight first iterations of the weighted reconstruction procedure when an area B enclosing the structures causing acoustic distortions can be determined *a priori*.

4. RESULTS

The results of the experiment described in section 3 are displayed in Figs. 1 and 2. Fig. 1 shows the results of the first eight iterations when no information regarding the distribution of acoustic reflectors is available. Generally, no significant improvement is achieved after the second iteration and some artefacts remain in the central region of the image. The reconstruction can be improved when an area B enclosing the structures causing acoustic distortion is *a priori* known (dashed circle in Fig. 2). The eight first iterations obtained in this case are showcased in Fig. 2. Again, no significant changes are perceived after the second iteration but the artefacts in the central region of the image are removed.

5. CONCLUSIONS

In this work, we have described a statistically-based weighting procedure for optoacoustic tomographic reconstructions in order to minimize the artefacts associated to internal ultrasonic scattering and reflections. Thereby, the optoacoustic signals are weighted with the probability that a reflected or scattered ultrasonic wave is measured, so that signals that are less likely to be affected by these acoustic phenomena have a higher contribution to the reconstruction. As the estimation of the probability that a reflected or scattered wave is detected depends on the optical absorption distribution, it is recalculated iteratively by considering that the reconstructed image in each iteration represents such optical absorption distribution. Furthermore, if the approximate location of the acoustic scatterers is determined *a priori*, the artefacts can further be reduced.

ACKNOWLEDGMENTS

Daniel Razansky acknowledges support from the German Research Foundation (DFG) Research Grant (RA 1848/1) and the ERC Starting Independent Researcher Grant. Vasilis Ntziachristos acknowledges support from the ERC Senior Investigator Award and the Medizin Technik BMBF award for excellence in medical innovation.

REFERENCES

[1] Wang, L. V. and Wu, H. I., [*Biomedical Optics: Principles and Imaging*], John Wiley & Sons, New Jersey (USA) (2007).

[2] Weissleder, R. and Pittet, M., "Imaging in the era of molecular oncology," *Nature* **452**(7187), 580–589 (2008).

[3] Beard, P., "Biomedical photoacoustic imaging," *Interface Focus* **1**(4), 602–631 (2011).

[4] Wang, L. V. and Hu, S., "Photoacoustic tomography: in vivo imaging from organelles to organs," *Science* **335**(6075), 1458–1462 (2012).

[5] Kruger, R. A., Liu, P., Fang, Y. R., and Appledorn, C. R., "Photoacoustic ultrasound (paus) - reconstruction tomography," *Medical Physics* **22**(10), 1605–1609 (1995).

[6] Paltauf, G., Viator, J. A., Prahl, S. A., and Jacques, S. L., "Iterative reconstruction algorithm for optoacoustic imaging," *Journal of the Acoustical Society of America* **112**(4), 1536–1544 (2002).

[7] Deán-Ben, X. L., Buehler, A., Ntziachristos, V., and Razansky, D., "Accurate model-based reconstruction algorithm for three-dimensional optoacoustic tomography," *IEEE Transactions on Medical Imaging* **31**(10), 1922–1928 (2012).

[8] Xu, M. and Wang, L. V., "Universal back-projection algorithm for photoacoustic computed tomography," *Physical Review E* **71**(1), 016706 (2005).

[9] Deán-Ben, X. L., Ma, R., Razansky, D., and Ntziachristos, V., "Statistical approach for optoacoustic image reconstruction in the presence of strong acoustic heterogeneities," *IEEE Transactions on Medical Imaging* **30**(2), 401–408 (2011).

[10] Xu, Y. and Wang, L. V., "Effects of acoustic heterogeneity in breast thermoacoustic tomography," *IEEE Transactions on Ultrasonics, Ferroelectrics and Frequency Control* **50**(9), 1134–1146 (2003).

[11] Manohar, S., Willemink, R. G. H., van der Heijden, F., Slump, C. H., and van Leeuwen, T. G., "Concomitant speed-of-sound tomography in photoacoustic imaging," *Applied Physics Letters* **91**(13), 131911 (2007).

[12] Deán-Ben, X. L., Razansky, D., and Ntziachristos, V., "The effects of acoustic attenuation in optoacoustic signals," *Physics in Medicine and Biology* **56**(18), 6129–6148 (2011).

[13] Treeby, B. E., "Acoustic attenuation compensation in photoacoustic tomography using time-variant filtering," *Journal of Biomedical Optics* **18**(3), 036008 (2013).

[14] Deán-Ben, X. L., Ntziachristos, V., and Razansky, D., "Statistical optoacoustic image reconstruction using a-priori knowledge on the location of acoustic distortions," *Applied Physics Letters* **98**(17), 171110 (2011).

[15] Deán-Ben, X. L., Ntziachristos, V., and Razansky, D., "Artefact reduction in optoacoustic tomographic imaging by estimating the distribution of acoustic scatterers," *Journal of Biomedical Optics* **17**(11), 110504 (2012).

[16] Deán-Ben, X. L., Nziachristos, V., and Razansky, D., "Acceleration of optoacoustic model-based reconstruction using angular image discretization," *IEEE Transactions on medical imaging* **31**(5), 1154–1162 (2012).

[17] Razansky, D., Buehler, A., and Ntziachristos, V., "Volumetric real-time multispectral optoacoustic tomography of biomarkers," *Nature Protocols* **6**(8), 1121–1129 (2011).